Breakdown of Crystal Structure in Potato Starch During Gelatinization

PAUL J. JENKINS, ATHENE M. DONALD

Cavendish Laboratory, University of Cambridge, Madingley Road, Cambridge CB3 OHE, United Kingdom

Received 24 January 1997; accepted 1 April 1997

ABSTRACT: Using a synchrotron source, *in situ* small- and wide-angle X-ray studies of the gelatinization of 40% potato starch slurries were carried out. By determining how the crystallinity index changes with temperature, it is possible to follow the destruction of the crystals. Fitting the (100) peak of the starch structure has shown that the crystals change only slightly in dimension over the temperature range studied. The large-scale swelling which occurs during gelatinization is associated with amorphous regions of the starch granule structure. © 1997 John Wiley & Sons, Inc. J Appl Polym Sci **66:** 225–232, 1997

INTRODUCTION

With the increased emphasis on utilizing renewable resources, attention is turning to the possibility of using natural polymers in place of synthetic ones. Starch is a very common biopolymer building block, which already finds many applications outside that of the food industry. However, if it is to succeed as a thermoplastic material, it is important that its properties are as well understood as are those of conventional polymers and that its processing is optimized. Because it is laid down in plants for energy storage, the mesoscopic structure within the starch granule is complex and has developed to suit the plant's own needs. Our research is directed toward understanding how this structure breaks down during heating in water—the process known as gelatinization—which will be equally important for industrial and food end uses.

The starch granule is known to be semicrystalline, and this gives rise to birefringence when viewed between crossed polars. As the starch granules gelatinize and their structure is disrupted, this birefringence is lost. Many studies have attempted to characterize the point at which all birefringence is lost for a sample studied under an optical microscope. This point is termed the birefringence end-point temperature (BEPT). Whereas the loss of birefringence occurs over quite a large temperature range for the whole sample (a BEPT range of 56–64°C has been measured for 12% starch [w/w] suspensions of wheat and potato starches heated at 1.5°C/min [Ref. 1]), individual granules are observed to lose birefringence over a much smaller range, generally less than 1°C.[2]

The loss of birefringence is associated with the loss of long-range order and is therefore also associated with the loss of crystallinity. The loss of crystallinity can be followed by wide-angle X-ray scattering (WAXS) studies. Crystallinity loss was quantitatively correlated with thermal events (as measured by DSC) in a detailed study by Liu et al.[3] Cooke and Gidley[4] used NMR to measure the double-helix content and observed that crystalline and molecular order are lost concurrently during gelatinization. Further work included measurements of birefringence loss,[5] and it was demonstrated that birefringence loss started earlier and concluded earlier than molecular and crystalline order loss, as also found by Liu et al.[3] However, it should be recognized that in these studies measurements of order were made by post-mortem study, and not *in situ*, raising the possibility of

Correspondence to: A. M. Donald.
Contract grant sponsors: BBSRC; Dalgety plc.

Journal of Applied Polymer Science, Vol. 66, 225–232 (1997)
 CCC 0021-8995/97/020225-08

some uncertainties creeping into the quantitative results.

In this article, *in situ* studies of changes in the WAXS patterns of potato starch during gelatinization in excess water are presented. These data were obtained using a synchrotron source so that data can be collected in real time during the gelatinization process and changes in the WAXS pattern can be related to thermal events via concomitant DSC studies.[6] In addition, small-angle scattering (SAXS) data were simultaneously collected. In our previous work, we devised a model which allows these SAXS data to be well-fitted. This model invokes the existence of three kinds of regions within the starch granule—semicrystalline stacks consisting of alternating crystalline and amorphous lamellae embedded in amorphous growth rings[7,8]—and this approach can be used to rationalize the SAXS data gathered here.

EXPERIMENTAL

Potato starch, supplied as a gift from Dalgety plc, with a starting moisture content of 14.4% was used. Samples were studied as slurries at a water concentration of 40% (w/w). X-ray experiments were carried out on station 8.2 at the SRS (Daresbury). The experimental arrangement was described previously.[6,9] Heating was carried out using a heat-flux DSC. This was a modified Linkam THM microscope hot stage. The design and construction of this DSC was described in more detail in Ref. 10. Starch slurries in water were sealed in modified Du Pont DSC pans.

The experimental procedure for obtaining simultaneous SAXS/WAXS patterns was described previously,[6,11] and the reader is referred to these articles for full details. The WAXS patterns were detected by an Inel detector, and, simultaneously, the SAXS ($<\sim 6°\ 2\theta$) patterns were detected by a quadrant detector. For most experiments, the quadrant detector was positioned 3 m distant from the sample. For measurements on the (100) wide-angle diffraction line, the detector was repositioned at a distance of 1.4 m from the sample. For each sample, a measurement of the X-ray scattering at room temperature was taken first. Then, the DSC was programmed to heat from room temperature to 120°C at a heating rate of 5°C/min.

Data collected on the Inel detector was normalized to the intensity of the direct beam. The region of interest was chosen to include most of the major diffraction peaks. Values of the crystallinity index, based on the method of Wakelin,[12] were obtained from the gradient of a least-squares fitted line to a plot of $(I_u - I_a)_{2\theta}$ vs. $(I_c - I_a)_{2\theta}$, where I_u, I_a, and I_c are the scattered intensities at a given value of 2θ for the data set and for the amorphous and crystalline reference samples, respectively. These reference samples were chosen as the last (fully gelatinized) and first (ungelatinized) data points as a function of temperature, respectively, as described previously.[6] Small-angle scattering profiles were corrected as described previously.[7] Information concerning the changes occurring in long-range order during gelatinization was obtained using the method described in Ref. 13.

Crystallite-size measurement is only possible from diffraction peaks that are well separated—in this case, the (100) reflection. This reflection occurs at a scattering angle outside the range covered by the Inel detector, but careful experimental procedure permitted the use of the quadrant detector to record simultaneously the SAXS data and the very low angle WAXS data containing the single peak at around $6°\ 2\theta$. It is usually necessary to correct the observed diffraction peak width for broadening due to the experimental arrangement. However, the point collimated nature of the beam (0.3 mm vertical height), compared to the pixel size of the detector (0.4–0.5 mm), meant that the experimental broadening was negligible and could be ignored. Peak position (in 2θ), heights and widths at half-maximum were obtained by fitting a Gaussian function to the curve. This function took the form

$$y = m_1 + m_2 \exp\left[\frac{-(x - m_3)^2}{m_4^2}\right] \qquad (1)$$

where m_1 is the offset; m_2, the peak height; m_3, the peak position; and m_4, the peak width. Peak fitting was performed using the Kaleidograph program on the Macintosh. Crystallite sizes were then obtained by applying the Scherrer formula:

$$\beta_{hkl} = \frac{0.89\lambda}{D_{hkl} \cos \theta} \qquad (2)$$

where D_{hkl} is the crystal size perpendicular to the planes scattering; θ, the scattering angle; λ, the incident wavelength; and β_{hkl}, the full angular width at half-maximum intensity of the reflection.

Although DSC data could be obtained simultaneously with the SAXS/WAXS data, this cell yields rather noisy data and was used mainly as a

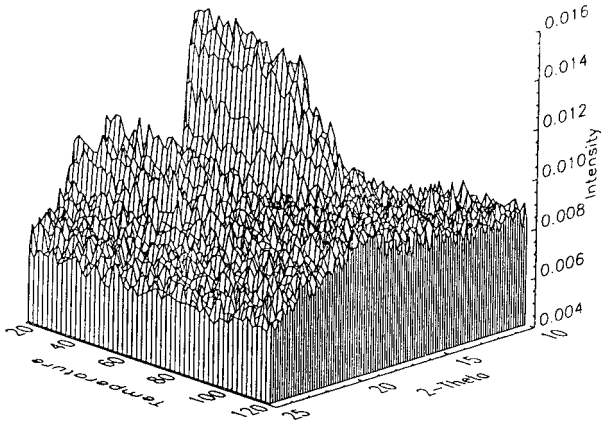

Figure 1 Wide-angle X-ray scattering profiles for 40% w/w potato starch in water as a function of temperature during gelatinization.

temperature calibration. More accurate DSC data were obtained outside the beam using a Perkin-Elmer DSC-7 equipped with an Intracooler II. Small (15–20 mg) samples of the starch slurry were hermetically sealed inside 50 μL aluminum pans and heated at 5°C/min. From the DSC trace, measurements were made of the start (T_s), onset (T_0), peak (T_p), and conclusion (T_c) temperatures. The start and conclusion temperatures are defined as the point at which the DSC trace first starts and finally ceases to deviate from a flat base line, respectively. The onset temperature is defined as the point at which a straight line drawn down the leading edge of the DSC endotherm intersects the base line. The peak temperature is defined as the point of maximum endothermic heat flow relative to the base line. Measurements of these values are based on the mean of three runs, with associated uncertainties of less than 1°C. The positions of these temperatures are marked on all subsequent plots.

RESULTS

Wide-angle X-ray diffraction patterns obtained *in situ* during gelatinization are shown in Figure 1. For these scattering patterns, we observed a steady reduction in the scattered intensity for the crystalline peaks. This occurs in parallel with a rise in the diffuse background scattering, suggesting an increase in the amount of amorphous material. Using the method of Wakelin,[12] the crystallinity index was determined for each temperature. Figure 2 shows the result of this analysis.

Concentrating now only on the (100) peak, using eq. (1), it is possible to determine how both the peak position and peak width vary with temperature. From knowledge of the peak position, it is possible to determine the interhelix separation within the amylopectin crystallites via the Bragg equation. Figure 3 shows how this separation increases with temperature. This increase corresponds to only an $\sim 0.1°$ shift in position. Determination of the peak width allowed the crystallite size to be determined in the (100) direction, from eq. (2), and the results are shown in Figure 4. This size corresponds to the lateral dimension of the crystallite, tangential to the axis of the lamellar stack[7] and tangential to the axis of the helices themselves. From these two measurements, it is possible to determine how the average number of double helices per crystallite varies with temperature, by dividing the average crystallite size by the average interhelix spacing. The results are shown in Figure 5.

Small-angle X-ray scattering patterns obtained in situ during gelatinization show, as in all our previous work,[6,7,13,14] a single peak, associated with the regular lamellar spacing within the granule. During gelatinization, this peak becomes less pronounced. However, at no time is it observed to shift in position. The intensity of scattering at all angles increases initially, before falling back. Using the model described previously,[6,7] we can obtain more detailed information by fitting each individual SAXS data set. As in the case of the gelatinization of wheat, of the six parameters in the model, only the two-electron density differences, $\Delta\rho$ (the difference in electron density between crystal ρ_c and amorphous lamellae ρ_a) and $\Delta\rho_u$ (the difference in electron density between amorphous lamellae and amorphous background ρ_u), change during gelatinization, with the bulk of the change occurring over the temperature range described by the DSC endotherm. The way these two parameters change over the temperature range is shown in Figure 6.

DISCUSSION

In Figure 1, we observe an initial gradual drop in the crystallinity index from room temperature until the onset of the DSC endotherm. After the onset temperature, the rate of crystallinity loss increases. At the conclusion temperature for the DSC endotherm, there still exists some residual

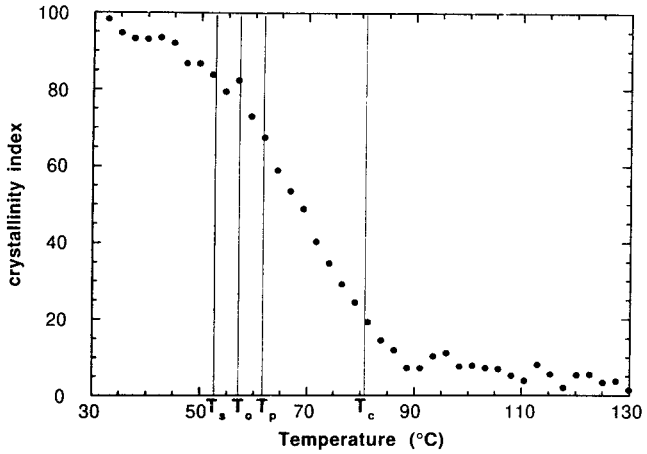

Figure 2 Variation in crystallinity index with temperature during gelatinization.

crystallinity. However, by around 90°, all crystallinity has been lost, and the crystallinity index reaches a flat base line, close to zero. This plot indicates that most (but not all) crystallinity loss occurs for temperatures within the gelatinization endotherm.

The shape of the crystallinity index curve is broadly consistent with that obtained for maize starch in an earlier study by Liu et al.[3] In both cases, starch gelatinized in excess water lost crystallinity over a wide range of temperatures. In the study by Liu et al., the measurements of the crystallinity index were not made *in situ*, but on preprepared partly gelatinized samples. As a result, direct correlation with DSC data was not possible. However, crystallinity index loss was accurately correlated with birefringence loss. It was observed that birefringence loss occurred over a much narrower range than did crystallinity loss and was completed well before all crystallinity had been lost. This observation is not unexpected, since birefringence requires structural ordering over a long range, whereas crystallinity can exist over a much shorter structural range. Consequently, the sample will lose birefringence when any part of the long-range order is disrupted, while crystallinity loss involves the disruption of smaller groupings of double helices. Our study supports these findings. In this study, the decrease in the crystallinity index occurred primarily between 57 and 90°C. For potato starch in excess water heated at 7°C/min, Leszczyñski[15] recorded birefringence loss in situ from 58–75°C. These results suggest that birefringence measurements, which are widely used to monitor polymer melting, provide only an approximation of the final melting point of starch polysaccharides. Furthermore, the observation made on a population of granules that the temperature range of crystallinity loss is much larger than the temperature

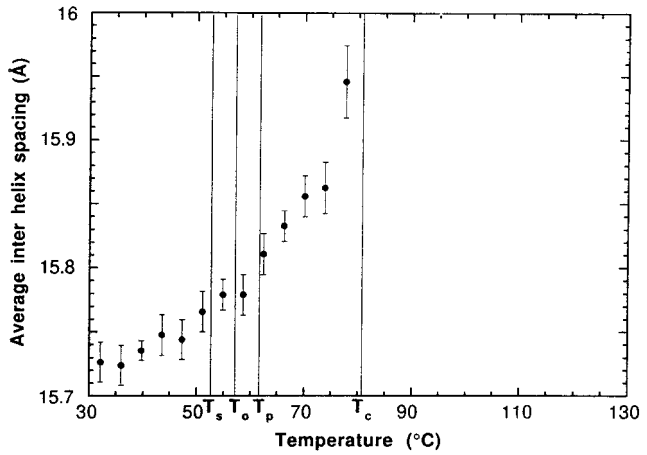

Figure 3 Changes in average interhelix spacing in (100) direction during gelatinization.

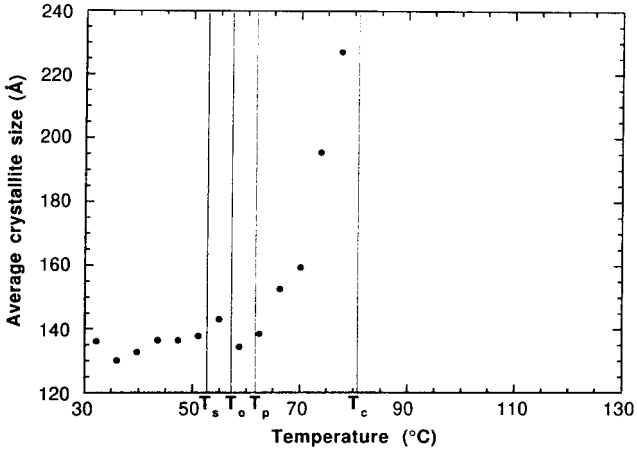

Figure 4 Changes in average crystallite size during gelatinization.

range of birefringence loss is likely to hold true for an individual granule. This calls into question the gelatinization range of 1°C measured by the birefringence loss for a single granule.[2] This observation, and the resulting conclusion that individual granules gelatinize highly cooperatively, is a central premise of the Evans and Haisman gelatinization model.[16]

It should also be noted that there is some reduction in the value of the crystallinity index from room temperature up to the onset point of the DSC endotherm. As argued before, this suggests that the initial drop in crystallinity index is due to changes within the amorphous as opposed to the crystalline regions of the granule.[6] The initial drop in the value of the crystallinity index would be consistent with an initial swelling of the amorphous regions of the granule. As these regions swell and increase in size, the crystallinity index (ratio of crystalline to amorphous material) would be reduced in value. This interpretation is supported by the observation that the peak height of the (100) peak does not start to fall until the onset of the DSC endotherm, indicating that the crystalline regions themselves are unchanged. Thereafter, the fall in peak height mirrors the crystallinity index decrease.

As shown in Figure 3, the average interhelix spacing in the (100) direction is observed to increase slightly during gelatinization. Most of this increase occurs within the temperature range spanned by the DSC endotherm. This increase in average interhelix spacing must be associated with a slight swelling of the crystallites tangential to the axis of the helices. However, the total swelling is only very slight, corresponding to an expansion of only 0.3 Å, or 2% relative to the initial interhelical spacing. For other spacings within

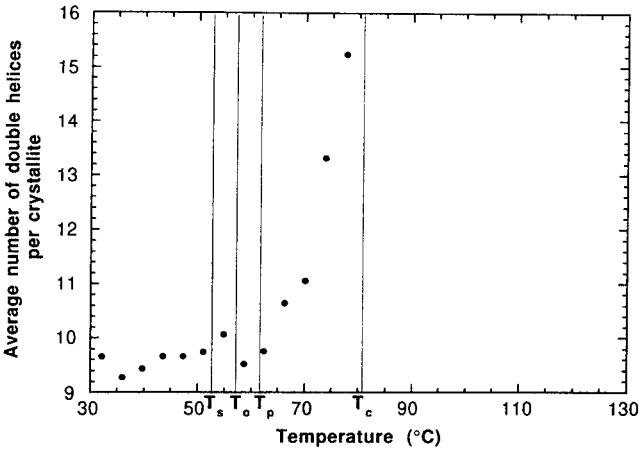

Figure 5 Change in average number of double helices per crystallite during gelatinization.

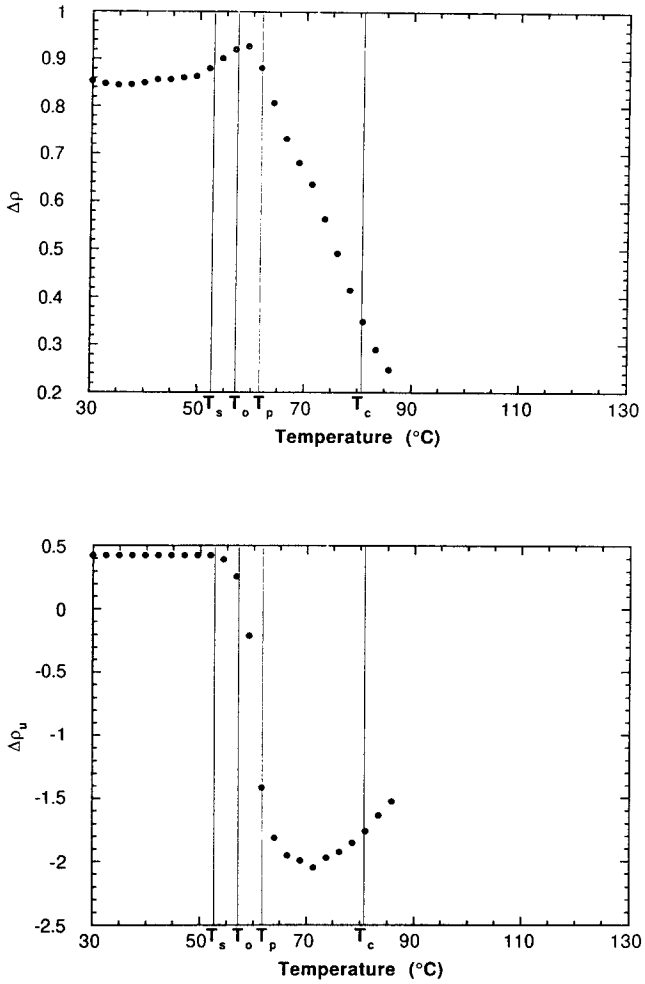

Figure 6 (a) Variation in $\Delta\rho$ with temperature. (b) Variation in $\Delta\rho_u$ with temperature.

the structure, it is not possible to measure exactly the changes in spacing taking place during gelatinization since all the other reflections overlap, preventing peak fitting of the kind used here. However, qualitative estimates suggest that neither the interhelical spacings nor the helical pitch change significantly during gelatinization. This observation suggests that the helices swell only very slightly in any direction during gelatinization.

The crystallite dimension in the (100) direction for potato starch was measured at 13.6 ± 0.2 nm at room temperature. This value represents the mean and standard deviation of three independent measurements. This value of 13.6 nm should be compared with the value of 14.7 nm obtained in an earlier WAXS study by Hizukuri and Nikuni.[17] Since this earlier study did not provide a value for the error on this measurement, it is difficult to compare the two measurements of crystallite size. However, they would seem to be broadly consistent with one another.

Figure 4 details the variation in average crystallite size during gelatinization. Initially, as the temperature is increased, the average crystallite size remains constant. However, in parallel with the crystallinity loss, after the peak of the DSC endotherm, we observe an increase in the average crystallite size. It is possible that this increase is a consequence of the slight swelling of the crystallites. Figure 5 details the change in the average number of double helices per crystallite as a function of temperature. If the increase in crystallite size was solely due to the tangential swelling of the crystallites, then the average number of double helices would remain constant during gelatinization. For temperatures below the peak of the DSC endotherm, the average number of double helices per crystallite remains constant, at around a value of 9. However, after the peak temperature

of the DSC endotherm, the average number of double helices per crystallite increases rapidly, with a final value of 16 at a temperature of 78°C [corresponding to the last measurable (100) peak]. This significant change in the average number of double helices per crystallite precludes the suggestion that the increase in average crystallite size is solely due to a tangential swelling of the crystallites.

It is unlikely that the increase in the average number of helices per crystallite is due to an aggregation of double helices during gelatinization. Instead, this change must be due to a change in the distribution of sizes of the crystallite. If the smaller crystallites are disrupted first during gelatinization, then the average number of helices per crystallite must increase. So, we conclude that smaller crystallites (containing few double helices) are less stable and suffer a disruption of their crystalline packing at lower temperatures than do larger crystallites (containing a large number of double helices). That small crystals are least stable is well known for other polymeric systems.[18]

With regard to the SAXS data, only the electron densities within the model were found to vary during gelatinization. All other structural parameters remained fixed at their pregelatinization values. It is significant that the average repeat distance between crystalline lamellae remains invariant. This invariance indicates that the semicrystalline lamellar stack, representing the semicrystalline growth ring, does not itself expand radially during gelatinization. Since the granule itself is known to exhibit quite pronounced radial expansion, we may conclude that this expansion is taking place solely within the amorphous background material, representing the amorphous growth ring. The lack of radial swelling observed for the semicrystalline growth ring is not entirely surprising, since any radial expansion would involve breaking many of the B chains in the amylopectin molecule and is therefore unlikely. This conclusion is consistent with the observation that the helical pitch does not change significantly during gelatinization. If the crystalline lamellae within the semicrystalline growth ring were expanding radially, we might expect to detect an increase in helical pitch.

Since the wide-angle data provide no evidence of any improvement in crystallite perfection taking place during gelatinization, the electron density of the crystalline lamellae is unlikely to increase. Consequently, the initial rise in $\Delta\rho$ (where $\Delta\rho = \rho_c - \rho_a$) seen in Figure 6(a) must be due to a reduction in the value of ρ_a. This may be the result of an increase in mobility of the amorphous branching chains within the amorphous lamellae, facilitating a small expansion of this region tangential to the lamellar stack axis. Shortly after the onset temperature, and just before the peak temperature of the DSC endotherm, the value of $\Delta\rho$ starts to fall. As the double helices dissociate, the electron density of the crystalline lamellae (ρ_c) also drops.

Further evidence to suggest an expansion of the amorphous growth ring is seen in the change in $\Delta\rho_u$ during gelatinization. $\Delta\rho_u$ is the difference in electron density between the amorphous background (density ρ_u) and the amorphous lamellae (density ρ_a), i.e., $\Delta\rho_u = \rho_u - \rho_a$. Figure 6(b) indicates that, starting around the start temperature of the DSC endotherm, the value $\Delta\rho_u$ drops rapidly and becomes increasingly negative up to a temperature of around 70°C. We have already concluded that ρ_a does not increase in value; consequently, the change in $\Delta\rho_u$ must be attributed to a fall in the value of ρ_u. A rapid drop in the value of ρ_u is consistent with the absorption of water into and the resultant expansion of the background region. This expansion would lead to a radial swelling of the granule. From 70°C upward, the value of $\Delta\rho_u$ slowly becomes less negative. Either the value of ρ_a is falling or that of ρ_u is increasing. The former effect could be associated with the disruption of the amorphous lamellae, with associated water uptake into this region. The latter effect could indicate the penetration of polysaccharide chains liberated from the semicrystalline growth ring into the amorphous growth ring. Since the density of this material is likely to be greater than that of the material within the amorphous growth ring, ρ_u would increase. It is difficult to be specific about structural changes taking place at these high temperatures, since by this point, much of the original internal structure of the granule has been disrupted.

The order of these events is for the initial rise in $\Delta\rho$ and the drop in $\Delta\rho_u$ to occur first, around the start temperature of the DSC endotherm. After the onset temperature, and before the peak temperature of the DSC endotherm, the value of $\Delta\rho$ starts to drop. This change continues to temperatures in excess of the conclusion temperature of the DSC endotherm. However, the big drop in $\Delta\rho_u$ is observed prior to the peak temperature of the DSC endotherm. Before the conclusion temperature of the DSC endotherm, $\Delta\rho_u$ has started to rise in value. The order of these events suggests that the rapid water uptake and associated radial

expansion within the background region is the trigger for the gelatinization process. In concert with this radial expansion, a small tangential expansion occurs within the amorphous lamellae. Since the amorphous background material is coupled to the semicrystalline lamellar stack, expansion of the amorphous background creates stresses within the semicrystalline lamellae. As these stresses increase, the double-helical crystallinity within the crystalline lamellae is disrupted.

These findings are broadly consistent with the Donovan[19] model for gelatinization in excess water. Using DSC to investigate the gelatinization behavior of potato starch, Donovan proposed a model whereby the swelling of the amorphous regions of the granule disrupted the crystalline order within the semicrystalline lamellae. Our study clearly confirms the link between swelling and crystallinity loss. In addition, we have pinpointed the location of the swelling to be predominantly within the amorphous growth ring rather than in the amorphous lamellae.

CONCLUSIONS

By studying the *in situ* gelatinization of potato starch by simultaneous SAXS/WAXS/DSC, it has been possible to show that the swelling of the granules which occurs during gelatinization is primarily associated with the amorphous growth rings. The semicrystalline lamellae stacks change hardly at all in dimension. However, as crystallinity loss proceeds, it is the smallest crystals which are destroyed first, leading to an increase in the average number of double helices per crystallite as the temperature is increased through the gelatinization range. The loss of crystallinity occurs over a wider temperature range than simply given by the DSC curves—which, in turn, has been previously shown to be occurring over a wider temperature range than was the birefringence loss.

The financial help of the BBSRC and Dalgety plc is gratefully acknowledged. We are grateful to Drs. Frazier and Bras for useful conversations.

REFERENCES

1. R. D. Hill and B. L. Dronzek, *Stärke,* **25,** 367–372 (1973).
2. D. French, in *Starch: Chemistry and Technology,* R. L. Whistler, J. N. BeMiller, and E. F. Paschall, Eds., Academic Press, New York, 1984, pp. 183–247.
3. H. Liu, J. Lelievre, and W. Ayong-Chee, *Carbohydr. Res.,* **210,** 79–87 (1991).
4. D. Cooke and M. J. Gidley, *Carbohydr. Res.,* **227,** 103–112 (1992).
5. M. J. Gidley and D. Cooke, *Biochem. Soc. Trans.,* **19,** 551 (1991).
6. P. J. Jenkins, R. E. Cameron, A. M. Donald, W. Bras, G. E. Derbyshire, G. R. Mant, and A. J. Ryan, *J. Polym. Sci. Phys. Ed.,* **32,** 1579–1583 (1994).
7. R. E. Cameron and A. M. Donald, *Polymer,* **33,** 2628–2635 (1992).
8. P. Jenkins, R. E. Cameron, and A. M. Donald, *Stärke,* **45,** 417–420 (1993).
9. W. Bras, G. E. Derbyshire, A. J. Ryan, G. R. Mant, F. Belton, R. A. Lewis, C. J. Hall, and G. M. Greaves, *Nuclear Instruments and Methods in Physics Research. Section A—Accelerators, Spectrometers, Detectors and Associated Equipment,* **326,** 587 (1993).
10. W. Bras, G. E. Derbyshire, A. Devine, S. M. Clark, J. Cooke, B. E. Komanschek, and A. J. Ryan, *J. Appl. Crystallogr.,* **28,** 26–32 (1995).
11. W. Bras, G. E. Derbyshire, A. J. Ryan, G. R. Mant, P. Manning, R. E. Cameron, and W. Mormann, *J. Phys. IV,* **3,** 447–450 (1993).
12. J. H. Wakelin, H. S. Virgil, and E. Crystal, *J. Appl. Phys.,* **30,** 1654–1662 (1959).
13. R. E. Cameron and A. M. Donald, *J. Polym. Sci. Phys. Ed.,* **31,** 1197–1204 (1993).
14. R. E. Cameron and A. M. Donald, *Carbohydr. Res.,* **244,** 225–236 (1993).
15. W. Leszczyñski, *Stärke,* **39,** 375 (1987).
16. I. Evans and D. Haisman, *Stärke,* **34,** 224–231 (1982).
17. S. Hizukuri and Z. Nikuni, *Nature,* **180,** 436–437 (1957).
18. D. C. Bassett, *Principles of Polymer Morphology,* Cambridge University Press, Cambridge, 1981.
19. J. Donovan, *Biopolymers,* **18,** 263 (1979).